Bonding of η^1-Acetylide Ligands to Electron-Rich Ruthenium Centers: Can Electron-Withdrawing Ligands Induce Significant Metal-to-Ligand Back-Bonding?

John E. McGrady,* Timothy Lovell, Robert Stranger, and Mark G. Humphrey

Department of Chemistry, The Australian National University, Canberra, ACT 0200, Australia

Received March 17, 1997[⊗]

The electronic structure of a series of η^1-acetylide complexes containing electron-rich ruthenium centers is examined using approximate density functional theory. Calculations are performed on two series of complexes, $Ru(C{\equiv}CR)(PH_3)_2(\eta^5\text{-}C_5H_5)$ and *trans*-$Ru(C{\equiv}CR)Cl(PH_3)_4$, with a series of substituted acetylide ligands, R = H, C_6H_5 and C_6H_4-4-NO_2. The π back-bonding ability of the ligands increases in the order R = H < C_6H_5 < C_6H_4-4-NO_2, while π donor properties vary as R = H < C_6H_4-4-NO_2 < C_6H_5. The cations of the complexes of the phenylacetylide ligand are therefore relatively stable, particularly when the vacancy at the metal center arises in an orbital coplanar with the phenyl π system. The nitrophenylacetylide ligand is a much weaker σ donor than either of the other two. Trends in calculated ionization energies result from a subtle interplay of changes in the σ donor, π donor, and π acceptor properties of the ligands and cannot be ascribed to one mechanism in isolation.

Introduction

Transition metal complexes containing η^1-acetylide ligands were first reported almost 30 years ago,[1] and since then they have remained an area of active research in organometallic chemistry.[2] The π system of the linear C≡C group provides a pathway for delocalization of electron density between the metal and ligand and, hence, an efficient mechanism for communication between two or more metal centers. Polymeric metal acetylides may, therefore, have potential applications in nonlinear optics,[3] where extensive mixing of ligand- and metal-based orbitals is necessary for a large nonlinear response,[4] in the development of conducting materials,[5] and also in artificial light-harvesting chromophores.[6] In light of the potential utility of these compounds, a detailed understanding of the nature of the metal−acetylide bond is clearly desirable.

Of particular interest is the extent to which the acetylide anion, isoelectronic with CO, participates in metal-to-ligand back-bonding.[7] Structural data are of limited value in addressing this question because of the relative insensitivity of the C≡C triple bond to small changes in population of the π or π^* orbitals. Consequently, the majority of C≡C bond lengths fall into a narrow range, and crystallographic data are often insufficiently precise for statistically significant trends to emerge.[2b,8] Metal−carbon bond lengths are potentially more susceptible to changes in back-bonding, but variations in the strength of the σ bond are likely to dominate the observed trends. Vibrational spectroscopy has been extensively utilized in metal carbonyl chemistry as a sensitive probe of back-bonding, the frequency of the intense C≡O vibrations falling as back-donation into the π^* orbital increases. The situation is, however, complicated in the acetylides, due to coupling of the C≡C stretch with vibrations associated with the terminal R group. Comparisons between different acetylides are, therefore, of limited value, and vibrational spectroscopy has also been unable to unequivocally establish back-bonding as a significant feature in the metal−acetylide bond.[9]

Photoelectron spectroscopy (PES), in conjunction with molecular orbital theory, is a valuable tool in analyzing

[⊗] Abstract published in *Advance ACS Abstracts,* August 1, 1997.

(1) (a) Jolly, P. W.; Pettit, R. *J. Organomet. Chem.* **1968**, *12*, 491. (b) Green, M. L. H.; Mole, T. *J. Organomet. Chem.* **1968**, *12*, 404.

(2) (a) Nast, R. *Coord. Chem. Rev.* **1982**, *47*, 89. (b) Manna, J.; John, K. D.; Hopkins, M. D. *Adv. Organomet. Chem.* **1995**, *38*, 79. (c) Stang, P. J.; Crittell, C. M. *Organometallics* **1990**, *9*, 3191. (d) Akita, M.; Terada, M.; Moro-oka, Y. *Organometallics* **1992**, *11*, 1825. (e) Bruce, M. I.; Humphrey, M. G.; Matisons, J. G.; Roy, S. K.; Swincer, A. G. *Aust. J. Chem.* **1984**, *37*, 1955. (f) Bruce, M. I.; Humphrey, M. G.; Snow, M. R.; Tiekink, E. R. T. *J. Organomet. Chem.* **1986**, *314*, 213.

(3) (a) Whittall, I. R.; Humphrey, M. G.; Hockless, D. C. R.; Skelton, B. W.; White, A. H. *Organometallics* **1995**, *14*, 3970. (b) McDonagh, A. M.; Whittall, I. R.; Humphrey, M. G.; Skelton, B. W.; White, A. H. *J. Organomet. Chem.* **1996**, *519*, 229. (c) McDonagh, A. M.; Whittall, I. R.; Humphrey, M. G.; Hockless, D. C. R.; Skelton, B. W.; White, A. H. *J. Organomet. Chem.* **1996**, *523*, 33. (d) Whittall, I. R.; Humphrey, M. G.; Samoc, M.; Swiatkiewicz, J.; Luther-Davies, B. *Organometallics* **1995**, *14*, 5493. (e) Whittall, I. R.; Humphrey, M. G.; Persoons, A.; Houbrechts, S. *Organometallics* **1996**, *15*, 1935. (f) Whittall, I. R.; Humphrey, M. G.; Houbrechts, S.; Persoons, A.; Hockless, D. C. R. *Organometallics* **1996**, *15*, 5378. (g) McDonagh, A. M.; Cifuentes, M. P.; Whittall, I. R.; Humphrey, M. G.; Samoc, M.; Luther-Davies, B.; Hockless, D. C. R *J. Organomet. Chem.* **1996**, *526*, 99. (h) Houbrechts, S.; Clays, K.; Persoons, A.; Cadierno, V.; Gamasa, M. P.; Gimeno, J.; Whittall, I. R.; Humphrey, M. G. *Proc. SPIE-Int. Soc. Opt. Eng.* **1996**, *2852*, 98. (i) Humphrey, M. G. *Chem. Aust.* **1996**, *63*, 442. (j) Whittall, I. R.; Humphrey, M. G.; Samoc, M.; Luther-Davies, B. *Angew. Chem., Int. Ed. Engl.* **1997**, *36*, 370. (k) Myers, L. K.; Langhoff, C.; Thompson, M. E. *J. Am. Chem. Soc.* **1992**, *114*, 7560. (l) Fyfe, H. B.; Mlekuz, D.; Zargarian, D.; Taylor, N. J.; Marder, T. B. *J. Chem. Soc., Chem. Commun.* **1991**, 188.

(4) Calabrese, J. C.; Cheng, L.-P.; Green, J. C.; Marder, S. R.; Tam, W. *J. Am. Chem. Soc.* **1991**, *113*, 7227.

(5) (a) Canadell, E.; Alvarez, S. *Inorg. Chem.* **1984**, *23*, 573. (b) Frapper, G.; Kertesz, M. *Inorg. Chem.* **1993**, *32*, 732.

(6) (a) Stranger, R.; McGrady, J. E.; Arnold, D. P.; Lane, I.; Heath, G. A. *Inorg. Chem.* **1996**, *35*, 7791. (b) Lin, V. S.-Y.; DiMagno, S. G.; Therien, M. J. *Science* **1994**, *264*, 1105. (c) Gosper, J. J.; Ali, M. *J. Chem. Soc., Chem. Commun.* **1994**, 1707. (d) Wong, A.; Kang, P. C. W.; Tagge, C. D.; Leon, D. R. *Organometallics* **1990**, *9*, 1992.

(7) (a) Chatt, J.; Duncanson, L. A. *J. Chem. Soc.* **1953,** 2339. (b) Dewar, M. J. S.; Ford, G. P. *J. Am. Chem. Soc.* **1979**, *101*, 783. (c) Versluis, L.; Ziegler, T. *J. Chem. Phys.* **1988**, *88*, 322.

(8) (a) Hughes, D. L.; Leigh, G. J.; Jimenez-Tenorio, M.; Rowley, A. T. *J. Chem. Soc., Dalton Trans.* **1993**, 75. (b) Hills, A.; Hughes, D. L.; Jimenez-Tenorio, M.; Leigh, G. J. *J. Organomet. Chem.* **1990**, *391*, C41. (c) Field, L. D.; George, A. V.; Hambley, T. W. *Inorg. Chem.* **1990**, *29*, 4565.

S0276-7333(97)00212-4 CCC: $14.00

the electronic structure of organometallic complexes because it allows an estimate not only of the relative energies of the electronic levels but also of their distribution over the molecule. Lichtenberger and co-workers have been prominent in this field, reporting studies on a variety of iron acetylides.[10] In these systems, they concluded that both the π and π^* orbitals of the acetylide ligand lie significantly higher than the corresponding orbitals in CO, bringing the metal dπ manifold closer in energy to the filled C≡C π orbitals than to their antibonding counterparts. Consequently, the acetylide acts as a π donor ligand rather than as a π acceptor and in this sense is more similar to Cl^- than to CO. This picture is consistent with previous conclusions drawn on the basis of a wide variety of molecular orbital calculations.[5b,11−13] In contrast, an *ab initio* study on acetylide complexes of titanium[14] indicated that the metal 3d orbitals were too high in energy to interact with the occupied π orbitals but still not close enough to π^* to allow effective back-bonding, and in these systems the ligand was effectively π neutral.

Despite the absence of theoretical support for the presence of back-bonding in metal acetylides, some physical data have been interpreted on the basis of significant metal-to-ligand charge transfer. For example, features in the electronic spectrum of *trans*-W(C≡CR)(≡CH)(dmpe)$_2$ have been used to infer significant back-bonding,[15] as has the ^{57}Fe Mössbauer spectrum of $[Fe(C{\equiv}CR)_6]^{4-}$.[16] The metal centers in these two species are more electron rich than those in the complexes described by Lichtenberger and coworkers,[10] suggesting that π back-bonding may become a significant feature of the metal−acetylide bond, given the correct combination of an electron-rich metal center and an electron-poor acetylide. In this paper, we present a computational study of electron-rich ruthenium acetylide complexes where a range of substituents on the acetylide modifies the electron-acceptor properties of the ligand. Specifically, we examine two series of model complexes, Ru(C≡CR)(PH$_3$)$_2$(η^5-C$_5$H$_5$) and *trans*-RuCl(C≡CR)(PH$_3$)$_4$ (R = H, C$_6$H$_5$ and C$_6$H$_4$-4-NO$_2$) (Scheme 1). Given the pivotal role of photoelectron spectroscopy in elucidating bonding trends, the major focus of our investigation will be to present a consistent interpretation of calculated ionization energies in terms of changes in metal−ligand bonding. In particular, we aim to determine whether trends in ionization energies induced by varying the acetylide ligand can be accounted for solely in terms of changes in back-bonding or whether a more subtle interplay of different electronic factors is at work.

Scheme 1. Structures of Ru(C≡CR)(PH$_3$)$_2$(η^5-C$_5$H$_5$) and *trans*-Ru(C≡CR)Cl(PH$_3$)$_4$ Complexes

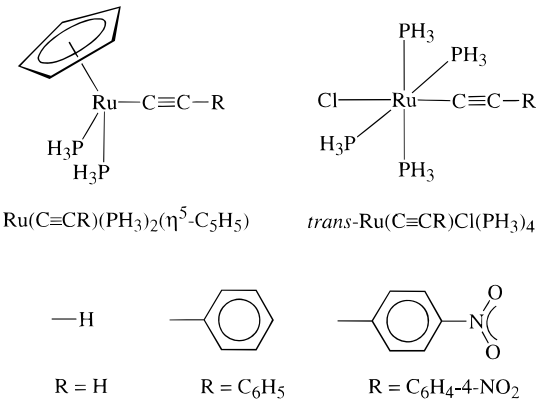

Computational Details

All calculations described in this paper are based on approximate DFT, (density functional theory), which has been applied to a wide variety of problems in organometallic chemistry.[17] Calculations were performed using the Amsterdam density functional (ADF) program developed by Baerends and co-workers.[18] The valence orbitals of the main group elements were expanded in double-ζ Slater-type basis sets, augmented with a single p-type polarization function for hydrogen and a single d function for carbon and phosphorus. The orbitals of ruthenium were represented by a triple-ζ basis.[19] An auxiliary set of s, p, d, f, and g Slater functions was used to fit the molecular electron density.[20] Electrons in orbitals up to and including 1s (C), 2p (P), and 4p (Ru) were considered as cores and treated using the frozen core approximation. The local exchange-correlation potential of Vosko, Wilk, and Nusair[21] was used in all cases, along with the gradient corrections of Becke[22] and Perdew.[23] Interaction energies were decomposed according to the generalized transition state approximation.[24] Geometries of the neutral *trans*-RuCl(C≡CR)(PH$_3$)$_4$ complexes were optimized in either C_{4v} (R = H) or C_{2v} (R = C$_6$H$_5$, C$_6$H$_4$-4-NO$_2$) symmetry using the gradient algorithm of Versluis and Ziegler.[25] The neutral Ru(C≡CR)(PH$_3$)$_2$(η^5-C$_5$H$_5$) complexes were optimized within C_s symmetry, with the arene ring lying in a plane bisecting the cyclopentadienyl group and the P−Ru−P angle, in accordance with the crystallographic data.[3a,26] Vertical ionization potentials were obtained by taking the difference between the

(9) (a) Grindley, T. B.; Johnson, K. F.; Katritsky, A. R.; Keogh, H. J.; Topsom, R. D. *J. Chem. Soc., Perkin Trans. 2* **1974**, 273. (b) Dale, J. In *Chemistry of Acetylenes*; Viehe, H., Ed.; Marcel Decker: New York, 1969.

(10) (a) Schilling, B. E. R.; Hoffmann, R.; Lichtenberger, D. L. *J. Am. Chem. Soc.* **1979**, *101*, 585. (b) Lichtenberger, D. L.; Renshaw, S. K.; Bullock, R. M. *J. Am. Chem. Soc.* **1993**, *115*, 3276. (c) Lichtenberger, D. L.; Renshaw, S. K.; Wong, A.; Tagge, C. D. *Organometallics* **1993**, *12*, 3522. (d) Lichtenberger, D. L.; Kellogg, G. E. *Acc. Chem. Res.* **1987**, *20*, 379.

(11) Kostic, N. M.; Fenske, R. F. *Organometallics* **1982**, *1*, 974.

(12) Louwen, J. N.; Hengelmolen, R.; Grove, D. M.; Oskam, A.; DeKock, R. L. *Organometallics* **1984**, *3*, 908.

(13) Khan, M. S.; Kakkar, A. K.; Ingham, S. L.; Raithby, P. R.; Lewis, J.; Spencer, B.; Wittmann, F.; Friend, R. H. *J. Organomet. Chem.* **1994**, *472*, 247.

(14) Knight, E. T.; Myers, L. K.; Thompson, M. E. *Organometallics* **1992**, *11*, 3691.

(15) Birchall, T.; Myers, R. D. *Spectrosc. Int. J.* **1983**, *2*, 22.

(16) Manna, J.; Geib, S. J.; Hopkins, M. D. *J. Am. Chem. Soc.* **1992**, *114*, 9199.

(17) (a) Ziegler, T. *Chem. Rev.* **1991**, *91*, 651. (b) Ziegler, T. *Pure Appl. Chem.* **1991**, *63*, 873. (c) Branchadell, V.; Deng, L.; Ziegler, T. *Organometallics* **1994**, *13*, 3115. (d) Woo, T. K.; Fan, L.; Ziegler, T. *Organometallics* **1994**, *13*, 2252. (e) Bickelhaupt, F. M.; Ziegler, T.; von Ragué Schleyer, P. *Organometallics* **1995**, *14*, 2288. (f) Fan, L.; Krzywicki, A.; Somogyvari, A.; Ziegler, T. *Inorg. Chem.* **1994**, *33*, 5287. (g) Ziegler, T. *Can. J. Chem.* **1995**, *73*, 743. (h) McGrady, J. E.; Stranger, R.; Bown, M.; Bennett, M. A. *Organometallics* **1996**, *15*, 3109.

(18) (a) Baerends, E. J.; Ellis, D. E.; Ros, P. *Chem. Phys.* **1973**, *2*, 42. (b) Baerends, E. J.; Ros, P. *Chem. Phys.* **1973**, *2*, 52. (c) Baerends, E. J.; Ros, P. *Int. J. Quantum Chem.* **1978**, *S12*, 169.

(19) Vernooijs, P.; Snijders, G. J.; Baerends, E. J. Slater Type Basis Functions for the Whole Periodic System. Internal Report; Free University of Amsterdam: Amsterdam, The Netherlands, 1981.

(20) Krijn, J.; Baerends, E. J. Fit Functions in the HFS Method. Internal Report; Free University of Amsterdam: Amsterdam, The Netherlands, 1984.

(21) Vosko, S. H.; Wilk, L.; Nusair, M. *Can. J. Phys.* **1980**, *58*, 1200.

(22) Becke, A. D. *Phys. Rev. A* **1988**, *38*, 3098.

(23) Perdew, J. P. *Phys. Rev. B* **1986**, *33*, 8822.

(24) (a) Ziegler, T.; Rauk, A. *Theor. Chim. Acta* **1977**, *46*, 1. (b) Ziegler, T.; Rauk, A. *Inorg. Chem.* **1979**, *18*, 1558. (c) Ziegler, T.; Rauk, A. *Inorg. Chem.* **1979**, *18*, 1755.

(25) Versluis, L.; Ziegler, T. *J. Chem. Phys.* **1988**, *88*, 322.

(26) Wisner, J. M.; Bartczak, T. J.; Ibers, J. A. *Inorg. Chim. Acta* **1985**, *100*, 115.

Table 1. Comparison of Calculated and Experimental Structural Data for Ru(C≡CR)(PR′$_3$)$_2$(η^5-C$_5$H$_5$) and *trans*-Ru(C≡CR)Cl(PP)$_4$

		Ru−C (Å)		C≡C (Å)	
	R	calculated	experimental	calculated	experimental
Ru(C≡CR)(PR′$_3$)$_2$(η^5-C$_5$H$_5$)	H	2.03		1.23	
	C_6H_5	2.00	1.994(5)[a]	1.23	1.202(8)[a]
			2.016(3)[b]		1.215(4)[b]
	C_6H_4-4-NO_2	1.99	1.99(2)[a]	1.23	1.23(2)[a]
			1.989(7)[b]		1.224(10)[b]
trans-Ru(C≡CR)Cl(PP)$_4$	H	2.06	1.906(9)[c]	1.22	1.162(9)[c]
	C_6H_5	2.05	2.007(5)[d]	1.23	1.198(7)[d]
	C_6H_4-4-NO_2	2.01	1.998(7)[e]	1.23	1.190(8)[e]

[a] R′ = Me.[3a] [b] R′ = Ph.[26] [c] PP = 1,2-bis(diphenylphosphino)methane (dppm).[27] [d] PP = 1,2-bis(diphenylphosphino)ethane (dppe).[28] [e] PP = 1,2-bis(diphenylphosphino)methane (dppm).[29]

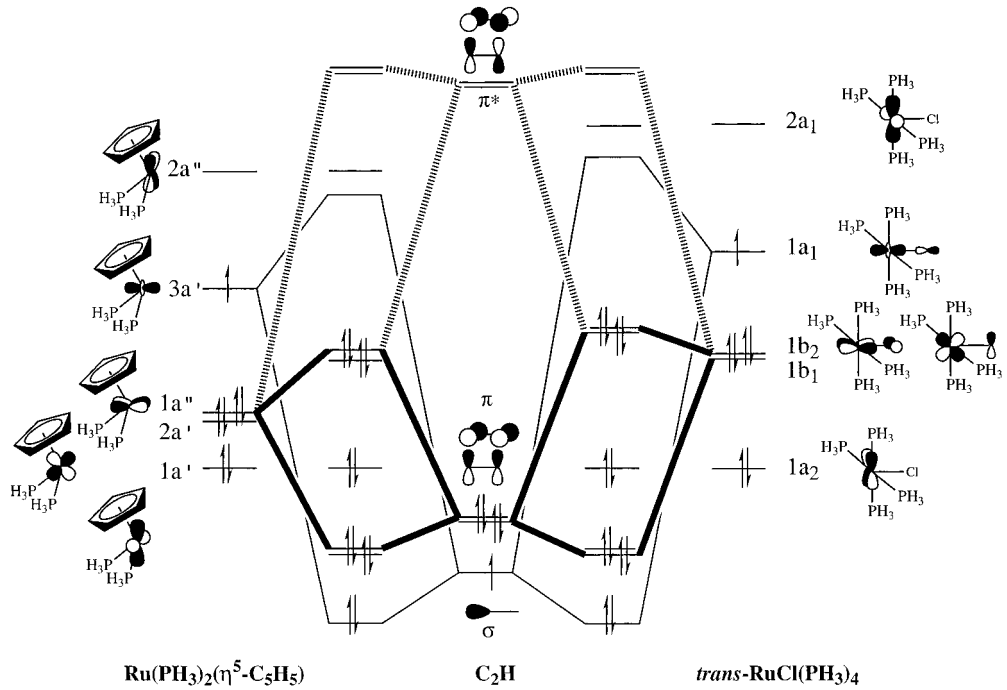

Figure 1. Comparative molecular orbital diagram for Ru(C≡CH)(PH$_3$)$_2$(η^5-C$_5$H$_5$) and *trans*-Ru(C≡CR)Cl(PH$_3$)$_4$.

ionized and ground-state energies at the equilibrium geometry (ΔSCF (self-consistent field) method).

Results and Discussion

Structural Data. Optimized structures of Ru(C≡CR)(PH$_3$)$_2$(η^5-C$_5$H$_5$) and *trans*-Ru(C≡CR)Cl(PH$_3$)$_4$ are compared to available crystallographic data in Table 1. The calculated Ru−C and C≡C bond lengths lie in the range 1.99−2.06 and 1.22−1.23 Å, respectively, in excellent agreement with majority of the experimental data. The only exception to this is the unusually short Ru−C bond length of 1.906(9) Å reported for *trans*-Ru(C≡CH)Cl(dppm)$_2$,[27] which contrasts markedly with the calculated value of 2.06 Å for *trans*-Ru(C≡CH)Cl(PH$_3$)$_4$ and also with all other crystallographically determined Ru−C bond lengths. The current DFT calculations are, therefore, unable to offer a simple explanation for the remarkable structure of *trans*-Ru(C≡CH)Cl(dppm)$_2$. Calculated C≡C bond lengths are notably invariant to modifications of the acetylide ligand, indicating that the triple bond is essentially unaffected by subtle electronic changes in the R group. In contrast, there is a distinct trend toward shorter Ru−C bond lengths for the nitrophenylacetylide systems, consistent with increased back-bonding where the ligand is more electron withdrawing. However, as noted by Hopkins and co-workers,[2b] the trend could also be caused by changes in the polarity of the Ru−C σ bond and so the structural data does not conclusively establish back-bonding as a significant feature of the Ru−C bond.

Ground-State Electronic Structure of Ru(C≡CH)(PH$_3$)$_2$(η^5-C$_5$H$_5$). The electronic structure of a Ru(PH$_3$)$_2$(η^5-C$_5$H$_5$) fragment, shown in Figure 1, is essentially that of a square pyramidal ML$_5$ fragment, with the η^5-C$_5$H$_5$ ring occupying three facially-disposed coordination sites.[10a] The singly occupied orbital, 3a′, is composed principally of metal d$_{z^2}$, and overlap with the sp-hybridized σ orbital of C≡CH forms the Ru−C σ bond. Of the three orbitals related to the t$_{2g}$ subset of an octahedron, two have approximate π symmetry with respect to the metal−acetylide axis (2a′, 1a″, the dπ subset) while the other has approximate δ symmetry (1a′, denoted dδ). Interactions between the metal dπ and occupied ligand π orbitals will destabilize the dπ

(27) (a) Touchard, D.; Haquette, P.; Pirio, N.; Toupet, L.; Dixneuf, P. H. *Organometallics* **1993**, *12*, 3132. (b) Khan, M. S.; Kakkar, A. K.; Ingham, S. L.; Raithby, P. R.; Lewis, J. *J. Organomet. Chem.* **1994**, *472*, 247.

(28) Faulkner, C. W.; Ingham, S. L.; Khan, M. S.; Lewis, J.; Long, N. J.; Raithby, P. R. *J. Organomet. Chem.* **1994**, *482*, 139.

(29) Hodge, A. J.; Ingham, S. L.; Kakkar, A. K.; Khan, M. S.; Lewis, J.; Long, N. J.; Parker, D. G.; Raithby, P. R. *J. Organomet. Chem.* **1995**, *488*, 205.

Scheme 2. Interaction of Acetylide and Arene π Systems

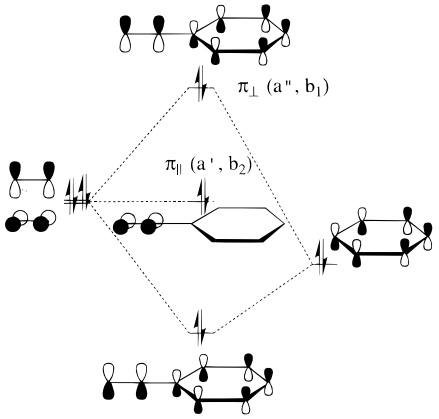

manifold relative to dδ, while interactions with the vacant ligand π^* orbital have the opposite effect, stabilizing dπ. In the remainder of this paper, we will refer to interactions between the metal dπ and ligand π orbitals as "forward-bonding" to distinguish them from the "back-bonding" interactions between dπ and ligand π^* orbitals. Unfortunately, forward- and back-bonding cannot be separated on symmetry grounds, as both ligand π and π^* orbitals have the same symmetry properties and either or both can interact with the metal dπ orbitals. In the schematic representation shown in Figure 1, the forward-bonding (solid line) is shown as the dominant feature, resulting in destabilization of the dπ orbitals, with back-bonding into the π^* manifold (broken line) of secondary importance. A major aim of this work is to provide quantitative estimates of the relative significance of the two processes, both in the ground and ionized states.

Ground-State Electronic Structure of *trans*-Ru(C≡CH)Cl(PH$_3$)$_4$. The principle features of the electronic structure of the *trans*-RuCl(PH$_3$)$_4$ fragment are very similar to those of Ru(PH$_3$)$_2$(η^5-C$_5$H$_5$). The t_{2g}-type orbitals may again be separated into distinct dπ ($1b_1$ and $1b_2$) and dδ ($1a_2$) subsets on the basis of their symmetry with respect to the Ru−C axis. The dπ subset are degenerate in the full C_{4v} symmetry of the isolated fragment but split into b_1 and b_2 representations in the C_{2v} symmetry prevalent in the arene-substituted acetylide complexes (R = C$_6$H$_5$, C$_6$H$_4$-4-NO$_2$) and are labeled accordingly in Figure 1. The separation between the dπ and dδ subsets is greater in *trans*-RuCl(PH$_3$)$_4$ relative to that in Ru(PH$_3$)$_2$(η^5-C$_5$H$_5$), as a result of antibonding interactions between dπ and the pπ orbitals of the chloride ion.

Influence of Arene Substituents. The addition of an arene ring to the acetylide group removes the 2-fold degeneracy of both the π and π^* orbitals. One component of each lies perpendicular to the plane of the ring (denoted $\pi_\perp$) and, consequently, is able to interact with the arene π system, while the other lies in the plane of the ring ($\pi_{||}$) and, therefore, remains essentially unperturbed by the substituent (Scheme 2). The transformation properties of $\pi_\perp$ and $\pi_{||}$, along with those of the metal-based orbitals, on descent in symmetry from C_{4v} → C_{2v} → C_s are summarized in Table 2. The higher symmetry of the *trans*-Ru(C≡CR)Cl(PH$_3$)$_4$ complexes (C_{4v} for R = H, C_{2v} for R = C$_6$H$_5$, C$_6$H$_4$-4-NO$_2$) relative to Ru(C≡CR)(PH$_3$)$_2$(η^5-C$_5$H$_5$) (C_s in all cases) simplifies

Table 2. Transformation Properties of Metal- and Ligand-Based Orbitals

	C_{4v}	C_{2v}	C_s
	Metal-Based Orbitals		
M dσ	a_1	a_1	a′
M dπ	e	$b_1 + b_2$	a′ + a″
M dδ	b_2	a_2	a′
	Ligand-Based Orbitals		
$\pi_\perp$, $\pi_\perp^*$	e	b_1	a″
$\pi_{||}$, $\pi_{||}^*$	e	b_2	a′

the analysis of the π bonding considerably. The most significant point to note is the complete separation, on symmetry grounds, of the Ru−C σ (a_1), $\pi_\perp$ (b_1), $\pi_{||}$ (b_2), and δ (a_2) interactions in the complexes of *trans*-RuCl(PH$_3$)$_4$. In contrast, for C_s symmetry, the $\pi_{||}$ orbitals have the same transformation properties as σ and δ (a′). It is for these symmetry reasons that we focus the forthcoming quantitative analysis on the *trans*-Ru(C≡CR)Cl(PH$_3$)$_4$ systems rather than the less symmetric Ru(C≡CR)(PH$_3$)$_2$(η^5-C$_5$H$_5$) series.

Quantitative Analysis of the Ruthenium−Carbon Interaction Energies. The Ru−C interaction energy, [Ru−C], can be decomposed using the generalized transition state approximation into separate terms arising from steric and orbital interaction terms, eq 1.[25]

$$[\mathrm{Ru-C}] = E_{\mathrm{st}} + E_{\mathrm{oi}} + E_{\mathrm{corr}} \quad (1)$$

The steric interaction term, E_{st}, arises through a combination of electrostatic interactions between the two fragments and destabilizing four-electron, two-orbital repulsions. Thus, any overlap between completely filled orbitals will make a destabilizing (positive) contribution to E_{st}. The orbital interaction energy, E_{oi}, is a result of the interaction of occupied orbitals on one fragment and vacant orbitals on the other and can be further subdivided into contributions from each irreducible representation of the point group. E_{corr} is a correction term accounting for the imperfect fit of the molecular electron density afforded by the auxiliary set of basis functions. In C_{2v} symmetry, the total energy may therefore be expressed as given in eq 2. [Ru−C]^0 is

$$[\mathrm{Ru-C}] = E_{\mathrm{st}} + Ea_1 + Ea_2 + Eb_1 + Eb_2 + E_{\mathrm{corr}} \quad (2)$$

defined as the interaction energy between a neutral *trans*-RuCl(PH$_3$)$_4$ fragment, configuration $(1a_2)^2(1b_2)^2(1b_1)^2(1a_1)^1$, and an acetylide radical, configuration $(\sigma)^1(\pi_\perp)^2(\pi_{||})^2$. For the ionized species, [Ru−C]$^{+a}$, [Ru−C]$^{+b}$, and [Ru−C]$^{+c}$ correspond to the interaction energy between the neutral ligand fragment and a cationic *trans*-RuCl(PH$_3$)$_4^+$ group with an electron removed from $1b_1$, $1b_2$, and $1a_2$, respectively. Total metal−ligand interaction energies ([Ru−C]) for the neutral ([Ru−C]^0) and ionized states ([Ru−C]$^{+a,b,c}$) of the three complexes are summarized in Table 3, along with their components defined according to eq 2.

In all cases, [Ru−C] is dominated by the component in a_1 symmetry, confirming that the Ru−C σ bond is the major stabilizing influence. Of more interest in the current context are the π interactions within the b_1 and b_2 representations, the sum of which ranges from −0.8 to −1.15 eV in the neutral complexes (Table 3). While this π bonding is clearly significant, it is important to emphasise that it represents only approximately 10% of the σ bond energy. Furthermore, the ligand-induced

Table 3. Components of [Ru−C] (eV) for Neutral and Ionized States of *trans*-Ru(C≡CR)Cl(PH$_3$)$_4$

R		E_{st}	Ea_1	Ea_2	Eb_1	Eb_2	E_{corr}	[Ru−C]
			[Ru−C]^0 $(1a_2)^2(1b_2)^2(1b_1)^2$					
H	all orbitals	+5.02	−10.03	0.00	−0.40	−0.40	+0.03	−5.78
	$-(\pi_\perp^*+\pi_\parallel^*)$	+5.02	−10.08	0.00	−0.03	−0.03	+0.02	−5.10
C_6H_5	all orbitals	+5.23	−10.21	0.00	−0.49	−0.42	+0.09	−5.80
	$-(\pi_\perp^*+\pi_\parallel^*)$	+5.23	−10.25	0.00	−0.04	−0.03	+0.06	−5.03
C_6H_4-4-NO_2	all orbitals	+5.75	−10.72	0.00	−0.65	−0.50	+0.08	−6.04
	$-(\pi_\perp^*+\pi_\parallel^*)$	+5.75	−10.76	0.00	−0.05	−0.04	+0.04	−5.06
			[Ru−C]$^{+a}$ $(1a_2)^2(1b_2)^2(1b_1)^1$					
H	all orbitals	+4.80	−9.62	0.00	−0.56	−0.36	−0.02	−5.76
	$-(\pi_\perp^*+\pi_\parallel^*)$	+4.80	−9.66	0.00	−0.33	−0.06	−0.03	−5.28
C_6H_5	all orbitals	+4.91	−9.79	0.00	−0.94	−0.38	−0.06	−6.26
	$-(\pi_\perp^*+\pi_\parallel^*)$	+4.91	−9.86	0.00	−0.62	−0.06	−0.06	−5.69
C_6H_4-4-NO_2	all orbitals	+5.69	−10.32	−0.01	−0.93	−0.45	−0.04	−6.06
	$-(\pi_\perp^*+\pi_\parallel^*)$	+5.69	−10.39	−0.01	−0.55	−0.07	−0.06	−5.39
			[Ru−C]$^{+b}$ $(1a_2)^2(1b_2)^1(1b_1)^2$					
H	all orbitals	+4.80	−9.62	0.00	−0.36	−0.56	−0.02	−5.76
	$-(\pi_\perp^*+\pi_\parallel^*)$	+4.80	−9.66	0.00	−0.06	−0.33	−0.03	−5.28
C_6H_5	all orbitals	+4.91	−9.71	−0.01	−0.41	−0.64	−0.02	−5.88
	$-(\pi_\perp^*+\pi_\parallel^*)$	+4.91	−9.78	−0.01	−0.07	−0.38	−0.03	−5.36
C_6H_4-4-NO_2	all orbitals	+5.69	−10.26	0.00	−0.48	−0.74	−0.05	−5.84
	$-(\pi_\perp^*+\pi_\parallel^*)$	+5.69	−10.33	−0.01	−0.08	−0.42	−0.05	−5.20
			[Ru−C]$^{+c}$ $(1a_2)^1(1b_2)^2(1b_1)^2$					
H	all orbitals	+4.75	−9.38	0.00	−0.33	−0.32	+0.02	−5.26
	$-(\pi_\perp^*+\pi_\parallel^*)$	+4.75	−9.44	0.00	−0.06	−0.06	+0.02	−4.79
C_6H_5	all orbitals	+4.87	−9.46	0.00	−0.36	−0.34	+0.04	−5.25
	$-(\pi_\perp^*+\pi_\parallel^*)$	+4.87	−9.54	0.00	−0.07	−0.06	+0.02	−4.78
C_6H_4-4-NO_2	all orbitals	+5.64	−10.00	0.00	−0.43	−0.40	+0.02	−5.17
	$-(\pi_\perp^*+\pi_\parallel^*)$	+5.64	−10.09	0.00	−0.08	−0.07	+0.01	−4.59

changes in π bonding (0.35 eV) represent a relative increase of only 3% of the corresponding σ bond strengths. Thus, it is important to realize that although we will discuss π bonding in some detail below, it is a comparatively minor component of the overall metal−ligand bond strength.

As noted earlier, the total orbital interaction energy in b_1 and b_2 symmetry is the sum of forward- and back-bonding components, and it is not possible to deconvolute the contribution of the two components simply on the basis of symmetry. It is, however, possible to determine the contribution of the back-bonding indirectly by repeating the fragment calculation described above after removing the vacant π^* orbitals of the ligand from the valence space. The residual interaction energy in b_1 and b_2 symmetry is then related to forward-bonding in isolation, while the difference between the two interaction energies (before and after removal of the π^* orbitals) provides a measure of the contribution of back-bonding. The components of [Ru−C] after removal of $\pi_\perp^*$ and $\pi_\parallel^*$ are also shown in Table 3. For example, where R = H, removal of the π^* orbitals effectively eliminates the attractive π interaction completely, reducing the energy in both b_1 and b_2 symmetry from −0.40 to −0.03 eV ([Ru−C]^0). The −0.03 eV is, therefore, a measure of the contribution of forward-bonding to the total interaction energy, whereas the difference between the two terms, −0.37 eV, represents the contribution of the metal-to-ligand back-bonding. The majority of the orbital interaction energy in π ($b_1 + b_2$) symmetry clearly arises through back-bonding, but it is important to emphasize that this does not necessarily indicate that the acetylide ligand is a poor π donor. For a Ru^{II} (d^6) ion the dπ subset is fully occupied, and therefore, overlap with the filled ligand π orbitals constitutes a destabilizing four-electron, two-orbital repulsion, the energetic contribution of which is found in E_{st} rather than E_{oi}. We will return to this important point in the disussion of the ionized species. The division of the π interactions (in both b_1 ($\pi_\perp$) and b_2 ($\pi_\parallel$) symmetry) into separate forward-bonding (fb) and back-bonding (bb) components is summarized in Table 4.

Table 4. Division of the π Interactions in *trans*-Ru(C≡CR)Cl(PH$_3$)$_4$ into Separate Contributions from Ligand-to-Metal Forward-Bonding (fb) and Metal-to-Ligand Back-Bonding (bb)

	Eb_1 (bb)	Eb_1 (fb)	Eb_2 (bb)	Eb_2 (fb)
	[Ru−C]^0 $(1a_2)^2(1b_2)^2(1b_1)^2$			
H	−0.37	−0.03	−0.37	−0.03
C_6H_5	−0.45	−0.04	−0.39	−0.03
C_6H_4-4-NO_2	−0.60	−0.05	−0.46	−0.04
	[Ru−C]$^{+a}$ $(1a_2)^2(1b_2)^2(1b_1)^1$			
H	−0.23	−0.33	−0.30	−0.06
C_6H_5	−0.32	−0.62	−0.32	−0.06
C_6H_4-4-NO_2	−0.38	−0.55	−0.38	−0.07
	[Ru−C]$^{+b}$ $(1a_2)^2(1b_2)^1(1b_1)^2$			
H	−0.30	−0.06	−0.23	−0.33
C_6H_5	−0.34	−0.07	−0.26	−0.38
C_6H_4-4-NO_2	−0.40	−0.08	−0.32	−0.42
	[Ru−C]$^{+c}$ $(1a_2)^1(1b_2)^2(1b_1)^2$			
H	−0.27	−0.06	−0.26	−0.06
C_6H_5	−0.29	−0.07	−0.28	−0.06
C_6H_4-4-NO_2	−0.35	−0.08	−0.33	−0.07

For R = H (C_{4v} symmetry), $\pi_\perp^*$ and $\pi_\parallel^*$ are degenerate and the π interaction is divided equally between the b_1 and b_2 representations (Table 3). The presence of an arene substituent on the acetylide ligand lifts this degeneracy, causing an asymmetric distribution of the total π interaction between b_1 and b_2. In b_2 symmetry, the $\pi_\parallel$ and $\pi_\parallel^*$ orbitals extend over the acetylide carbons only, and hence, the back-bonding is essentially unaffected by the arene substituent (Table 4). In b_1 symmetry, however, $\pi_\perp$ and $\pi_\perp^*$ overlap with the arene π system and substantial changes are induced by the substituent. There is a moderate (0.08 eV) increase in back-bonding upon addition of a phenyl group and a further 0.15 eV increase upon addition of the nitro group. The calculations, therefore, indicate that the

electron-withdrawing influence of the nitro group does indeed enhance the π back-bonding capability of the acetylide ligand. However, despite the fact that the absolute contribution of back-bonding increases by over 50% across the series, it is important to emphasize that it still represents at most 10% of the Ru−C σ bond energy and is, therefore, a minor effect in terms of the overall stability of the system.

Ionized Species. Conceptually, the simplest of the ionized states is the third, where the electron has been removed from the dδ orbital ($1a_2$), which is not directly involved in bonding to the acetylide ligand. Table 3 indicates that the major difference between $[Ru-C]^0$ and $[Ru-C]^{+c}$ is the reduced interaction within the a_1 representation, indicating that the Ru−C σ bond is weakened upon ionization. The influence of back-bonding is also reduced in the cation (Table 4), an effect which can be traced to the overall contraction and stabilization of the metal-based d orbitals upon ionization. Furthermore, the loss of back-bonding stabilization energy upon oxidation is approximately 40% in each system, and so the gross loss is greatest in the nitrophenylacetylide where back-bonding in the neutral complex is most prominent. Removal of an electron from either $1b_1$ or $1b_2$ creates a hole in the dπ manifold and, therefore, opens up a pathway for π donation from the acetylide ligand. Consequently, we anticipate that in addition to the background effects of removing an electron from an innocent orbital described above, a stabilizing contribution from π donation into the vacant site may arise. This qualitative expectation is borne out by the components of $[Ru-C]^{+a}$ and $[Ru-C]^{+b}$ shown in Tables 3 and 4. The background effects outlined for $[Ru-C]^{+c}$ (a decrease in the Ru−C σ bond strength and π back-bonding contributions) persist in both cations, but an additional stabilizing contribution from π forward-bonding is found in either b_1 ($[Ru-C]^{+a}$) or b_2 symmetry ($[Ru-C]^{+b}$), depending on where the vacancy in the dπ manifold is located. Furthermore, addition of a phenyl substituent causes greater changes in the Eb_1 (fb) term in $[Ru-C]^{+a}$ than in the Eb_2 (fb) term in $[Ru-C]^{+b}$. This observation is connected to the orientation of the ligand $\pi_\perp$ and $\pi_{||}$ orbitals described in Scheme 2. The $\pi_\perp$ orbital (b_1 symmetry) is delocalized over the phenyl π system, whereas the $\pi_{||}$ orbital (b_2) lies orthogonal to it. As a consequence, where the vacancy arises in a dπ orbital of b_1 symmetry ($[Ru-C]^{+a}$), the Eb_1 (fb) term in $[Ru-C]^{+a}$ increases markedly upon addition of a phenyl group and then decreases again upon addition of the nitro group. The electron-withdrawing nitro substituent clearly not only enhances the π acceptor properties of the acetylide, as discussed previously, but also diminishes the π donor ability of the ligand. In contrast, if the vacancy arises in the b_2 orbital ($[Ru-C]^{+b}$), forward-bonding (Eb_2 (fb)) is much less sensitive to the nature of the substituent, varying only by 0.09 eV across the series.

Ionization Energies. Calculated ionization potentials for Ru(C≡CR)$(PH_3)_2(\eta^5\text{-}C_5H_5)$ and *trans*-Ru(C≡CR)-$Cl(PH_3)_4$ are compared in Figure 2. Ionizations are labeled according to the orbital from which the electron is removed (see Figure 1). The third ionization for the *trans*-Ru(C≡CR)$Cl(PH_3)_4$ complexes lies relatively higher than that in the cyclopentadienyl series (note discontinuity in scale), due to the π donor properties of

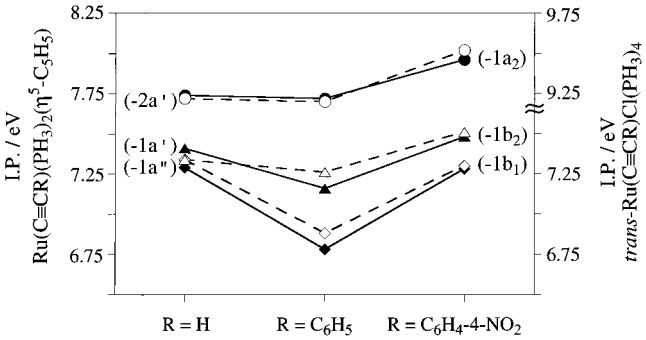

Figure 2. Calculated ionization potentials for Ru(C≡CR)-$(PH_3)_2(\eta^5\text{-}C_5H_5)$ (solid lines) and *trans*-Ru(C≡CR)$Cl(PH_3)_4$ (dashed lines).

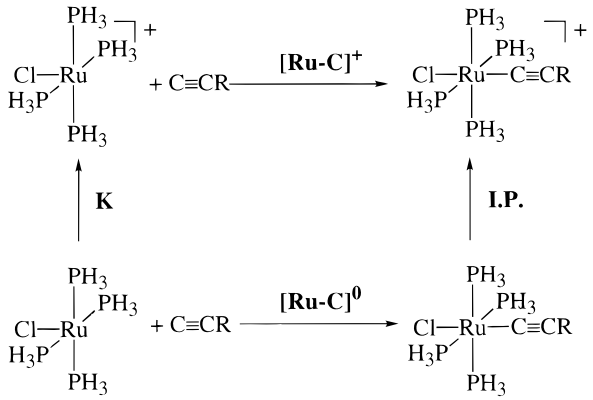

Figure 3. Relationship between ionization potential IP and Ru−C interaction energies ([Ru−C]) in neutral and ionized states.

the chloride ligand which strongly destabilize the dπ manifolds. Otherwise, the qualitative trends in ionization energies are remarkably independent of the nature of the metal center. The first and second ionization energies drop on addition of the phenyl substituent and then rise again when the nitro group is is added, the minimum at R = C_6H_5 being particularly prominent for the first ionization process. In contrast, the third ionization process is almost unaffected by addition of the phenyl group but again rises significantly when the phenyl group is replaced by the more electron-withdrawing nitrophenyl. The high ionization potentials for the nitrophenylacetylide systems are compatible with the idea of orbital stabilization caused by enhanced metal-to-ligand back-bonding. In the following section, we decompose the calculated ionization energies into distinct contributions from changes in σ and π bonding and examine the extent to which this conceptually simply model is substantiated by detailed analysis.

To interpret the trends in ionization potentials in terms of metal−ligand bonding, it is important to recognize that the energy of the process corresponds to the difference between the ground- and excited-state energies. Consequently, we must consider not simply the nature of the Ru−C bond in the ground or ionized states, but rather oxidation-induced *changes* in the bonding. From the energy cycle shown in Figure 3, the ionization potential may be expressed in terms of metal−ligand interaction energies as stated in eq 3, where ΔE[Ru−C] is defined as ($[Ru-C]^+ - [Ru-C]^0$).

$$\mathrm{IP} = K + \Delta E[\mathrm{Ru-C}] \qquad (3)$$

K is effectively constant for a given ionization process

Table 5. Relative Energies (eV) and Their Components for the First, Second, and Third Ionization Potentials of *trans*-Ru(C≡CR)Cl(PH$_3$)$_4$

R	ΔE_{st}	ΔEa$_1$	ΔEa$_2$	ΔEb$_1$ (bb)	ΔEb$_1$ (fb)	ΔEb$_2$ (bb)	ΔEb$_2$ (fb)	ΔE_{corr}	IP (rel)
				First Ionization Potential (−1b$_1$)					
H	−0.22	+0.41	0.00	+0.14	−0.30	+0.07	−0.03	−0.05	0.00
C_6H_5	−0.32	+0.42	0.00	+0.13	−0.58	+0.07	−0.03	−0.13	−0.46
C_6H_4-4-NO_2	−0.06	+0.40	−0.01	+0.22	−0.50	+0.08	−0.03	−0.12	−0.04
				Second Ionization Potential (−1b$_2$)					
H	−0.22	+0.41	0.00	+0.07	−0.03	+0.14	−0.30	−0.05	0.00
C_6H_5	−0.32	+0.50	−0.01	+0.11	−0.03	+0.13	−0.35	−0.11	−0.10
C_6H_4-4-NO_2	−0.06	+0.46	0.00	+0.20	−0.03	+0.14	−0.38	−0.13	+0.18
				Third Ionization Potential (−1a$_2$)					
H	−0.27	+0.65	0.00	+0.10	−0.03	+0.11	−0.03	0.00	0.00
C_6H_5	−0.36	+0.75	0.00	+0.16	−0.03	+0.11	−0.03	−0.05	+0.02
C_6H_4-4-NO_2	−0.11	+0.72	0.00	+0.25	−0.03	+0.13	−0.03	−0.06	+0.34

(variations of approximately 0.01 eV are caused by small changes in the optimized geometry of the molecule) and corresponds to the energy required to remove an electron from a specific orbital of the isolated metal fragment. The metal−ligand bond energies $[Ru-C]^{0/+}$ can then be further decomposed according to the generalized transition state approximation.[24] We have already illustrated the benefits of high symmetry in this form of analysis, and consequently, we restrict our discussion to the *trans*-Ru(C≡CR)Cl(PH$_3$)$_4$ systems. Given the similarities between these complexes and the Ru(C≡CR)(PH$_3$)$_2$(η^5-C$_5$H$_5$) systems (Figure 2), we are confident that conclusions based on analysis of the higher symmetry complexes can be extrapolated back to the cyclopentadienyl systems.

Combining eqs 2 and 3 leads to eq 4, where ΔE

$$\mathrm{IP} = K + \Delta E_{st} + \Delta E\mathrm{a}_1 + \Delta E\mathrm{a}_2 + \Delta E\mathrm{b}_1 + \Delta E\mathrm{b}_2 + \Delta E_{corr} \quad (4)$$

represents the ionization-induced *change* in a particular energy term, (E[Ru−C]$^+$ − E[Ru−C]^0). Further subdividing ΔEb$_1$ and ΔEb$_2$ into forward-bonding (fb) and back-bonding (bb) components leads to eq 5. The

$$\mathrm{IP} = K + \Delta E_{st} + \Delta E\mathrm{a}_1 + \Delta E\mathrm{a}_2 + \Delta E\mathrm{b}_1\,(\mathrm{fb}) + \Delta E\mathrm{b}_1\,(\mathrm{bb}) + \Delta E\mathrm{b}_2\,(\mathrm{fb}) + \Delta E\mathrm{b}_2\,(\mathrm{bb}) + \Delta E_{corr} \quad (5)$$

various components of the first ionization potential as defined in eq 5 are summarized in Table 5.

When considering the relative energies of the orbitals, and hence trends in ionization potentials, we must distinguish between a bulk shift in all metal-based orbitals (the charge potential effect), determined principally by the transfer of charge from ligand to metal, and shifts in the separation between the dπ and dδ orbitals (differential π effects). In terms of the analysis described above, we can equate the charge potential effects with a combination of the steric energy, E_{st}, and the interactions in σ symmetry (a$_1$), both of which affect the d$_\pi$ and d$_\sigma$ orbitals equally.

The third ionization potential, corresponding to removal of a dδ electron (−1a$_2$) serves as a base line for the interpretation of all three ionization processes, as the active orbital is not directly involved in Ru−C bonding. Comparing R = H with R = C_6H_5, we note that the ΔE_{st} term is reduced by 0.09 eV upon addition of the phenyl group, but this is offset by a similar increase in ΔEa$_1$. There is also a small increase in the ΔEb$_1$ (bb) term, indicating that the energetic contribution of back-bonding is marginally reduced in the cation. The net result of these small changes is that the third ionization potentials of the two systems are very similar. Changes on going from R = C_6H_5 to C_6H_4-4-NO_2 are more substantial, leading to a +0.32 eV rise in the ionization potential. Analysis of the various components indicates that in this case the major changes occur in the ΔE_{st} term, which is much higher (less negative) in the presence of the nitro group. As noted above, the steric term is associated with the charge potential effect, influencing all three metal-based orbitals approximately equally. Thus, we conclude that the much higher third ionization potential for R = C_6H_4-4-NO_2 is caused primarily by charge potential effects associated with the reduced ability of the nitrophenylacetylide ligand to donate charge in an inductive manner. The ΔEb$_1$ (bb) term is also somewhat larger in the nitrophenylacetylide system, reflecting the fact that back-bonding is most prominent in the neutral nitro-substituted system. However, the change in ΔEb$_1$ (bb) is still only 0.09 eV, less than 25% of the overall change in ionization potential, and hence, changes in back-bonding should be regarded as only a minor factor, enhancing the trend already established by the charge potential effects. Furthermore, an examination of Table 5 shows that the same patterns in ΔEb$_1$ (bb) emerge for each of the three ionization processes, indicating that rather than differentiating ionizations from the dπ and dδ orbitals, π back-bonding has an approximately equal influence in each case. In the discussion of the first and second ionization energies, the combined effects of changes in ΔE_{st} and ΔEb$_1$ (bb), which determine the relative positions of the third ionization potentials, are taken as a reference base line for the first and second ionization processes.

Having established the influence of the underlying charge potential, we can now proceed to analyze the more complex (in terms of metal−acetylide bonding) first and second ionization potentials, the relative positions of which are shown (relative to the reference base line) schematically in Figure 4. The second ionization process corresponds to removal of an electron from the b$_2$ orbital, which generates a vacancy in a metal-based orbital orthogonal to the phenyl π system. Accordingly, the cations are stabilized by the ΔEb$_2$ (fb) term, which increases upon addition of a phenyl substituent by 0.05 and 0.08 eV for R = C_6H_5 and C_6H_4-4-NO_2, respectively, confirming that the electron-releasing ability of the $\pi_{||}$ orbital is marginally enhanced by addition of a phenyl substituent. The changes between the third and second ionization potentials shown in Figure 4 can, therefore, be visualized as a marginal

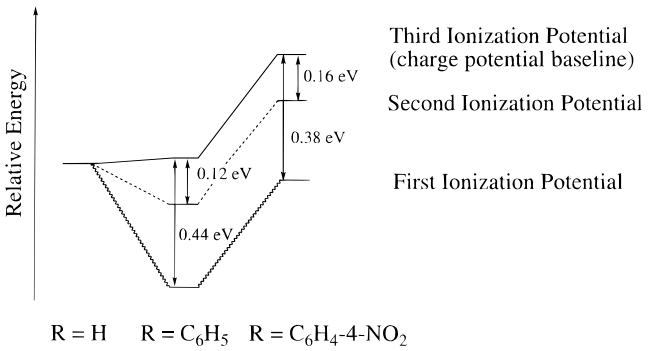

Figure 4. Relative positions of the first, second, and third ionization potentials *trans*-Ru(C≡CR)Cl(PH_3)$_4$.

downward shift of both phenyl- and nitrophenyl-substituted systems relative to R = H (0.12 and 0.16 eV, respectively), caused by the enhanced π donor properties of both ligands. The influence of the underlying charge potential base line can still be discerned by noting that the separation between the ionization potentials of R = C_6H_5 and C_6H_4-4-NO_2 remains approximately constant.

In contrast to the marginal effects noted above, the first ionization potential is highly ligand dependent because now the electron is removed from a dπ orbital coplanar with the phenyl π system ($1b_1$). As a result, π electron density from the phenyl ring can be donated to the cationic metal fragment, giving rise to a very large negative ΔEb_1 (fb) term for both R = C_6H_5 and C_6H_4-4-NO_2. The decrease of −0.28 eV between R = H and C_6H_5 should be contrasted with the much smaller −0.05 eV change in ΔEb_2 (fb) for the second ionization, where the vacant orbital lies orthogonal to the phenyl π system. When these changes are superimposed on the charge potential base line defined by the third ionization potentials, the enhanced π donor ability of the phenylacetylide leads directly to the much reduced ionization potential observed for R = C_6H_5 (in terms of Figure 4, both phenyl- and nitrophenyl-substituted systems are now shifted downwards substantially (*ca.* −0.40 eV) relative to R = H). For the nitrophenyl system, the large contribution from forward-bonding is just sufficient to counter the effects of the ΔE_{st} term and bring the ionization potential close to that for R = H.

Conclusions

In this paper we have used approximate DFT to study the influence of the substituent R on ruthenium−acetylide bonding in Ru(C≡CR)(PH_3)$_2$(η^5-C_5H_5) and *trans*-Ru(C≡CR)Cl(PH_3)$_4$. A series of three model acetylide ligands, C≡CR, is considered with R = H, C_6H_5, and C_6H_4-4-NO_2. Metal-to-ligand back-bonding increases in the order R = H < C_6H_5 < C_6H_4-4-NO_2, whereas ligand-to-metal forward-bonding increases in the order R = H < C_6H_4-4-NO_2 < C_6H_5. Thus, the addition of an electron-withdrawing nitro group enhances the π acceptor character of the acetylide ligand and also reduces its π-donor properties. In total magnitude, however, these π bonding effects are relatively small compared to the dominant influence of Ru−C σ bonding.

Trends in calculated ionization potentials have been analyzed in terms of oxidation-induced changes in the strength of the ruthenium−acetylide bond. The charge potential effects of the ligands, which influence all metal-based orbitals approximately equally, are established by considering the third ionization process, from a metal-based orbital not directly involved in metal−ligand π bonding. The electron-withdrawing nitro group greatly reduces the ability of the ligand to donate electron density through the σ framework, thereby stabilizing all metal-based orbitals. This, combined with the enhanced metal-to-ligand back-bonding, gives rise to a relatively high third ionization potential for the nitrophenylacetylide system. Where a vacancy is generated in the dπ manifold, additional stabilization for the cation can occur through donation of charge from the ligand π orbitals. This is most prominent when the vacant orbital is coplanar with the phenyl π system (first ionization), allowing extensive delocalization of the positive charge. The greater π donor ability of the phenyl and nitrophenylacetylide ligands results in a substantial stabilization of the cation relative to those in the protoacetylide, R = H. In the nitrophenylacetylide system, the weak σ donor properties of the ligand are, therefore, compensated by its relatively strong π donor ability, with the result that the first ionization potentials for *trans*-Ru(C≡CC_6H_4-4-NO_2)Cl(PH_3)$_4$ and *trans*-Ru(C≡CH)Cl(PH_3)$_4$ are very similar. In contrast, the strong π donor ability of R = C_6H_5 is not offset by weak σ donor character, and the first ionization potential of *trans*-RuCl(C≡CC_6H_5)(PH_3)$_4$ is significantly lower than either of the other two.

In summary, the calculated ionization potentials are the result of a subtle interplay of inductive charge donation and π forward- and back-bonding. All three factors vary considerably from ligand to ligand, and similar ionization potentials may arise through a cancellation of two terms. It would, therefore, be unwise to interpret trends in ionization potentials solely in terms of back-bonding without considering changes in the others.

Acknowledgment. We gratefully acknowledge the Australian Research Council (ARC) for financial support, and Professor Dennis L. Lichtenberger and Andrew Uplinger for helpful discussions. M.G.H. is an ARC Australian Research Fellow, and T.L. is supported by an EPSRC (U.K.) overseas studentship.

OM970212D